RESEARCH PAPER

# A missense mutation in *Large Grain Size 1* increases grain size and enhances cold tolerance in rice

Xiaolong Chen[1], [ID] , Liangrong Jiang[1], Jingsheng Zheng[1], Fangyu Chen[2], Tiansheng Wang[3], Meiling Wang[1], Yi Tao[1], Houcong Wang[1], Zonglie Hong[1,4,*], Yumin Huang[1,*] and Rongyu Huang[1,*]

[1] School of Life Sciences, Xiamen University, Xiamen 361102, China
[2] Key Laboratory of Ministry of Education for Genetics, Breeding and Multiple Utilization of Crops, College of Crop Science, Fujian Agriculture and Forestry University, Fuzhou 350002, China
[3] Quanzhou Institute of Agricultural Sciences, Quanzhou 362212, China
[4] Department of Plant Sciences, University of Idaho, Moscow, ID 83844, USA

* Correspondence: zhong@uidaho.edu, hym@xmu.edu.cn, and huangrongyu@xmu.edu.cn

## Abstract

Grain shape is controlled by quantitative trait loci (QTLs) in rice (*Oryza sativa* L.). A rice mutant (JF178) with long and large grains has been used in a breeding program for over a decade, but its genetic basis has been unclear. Here, a semi-dominant QTL, designated *Large Grain Size 1* (*LGS1*), was cloned and the potential molecular mechanism of *LGS1* function was studied. Near-isogenic lines (NILs) and a map-based approach were employed to clone the *LGS1* locus. *LGS1* encodes the OsGRF4 transcription factor and contains a 2 bp missense mutation in the coding region that coincides with the putative pairing site of miRNA396. The *LGS1* transcript levels in the mutant line were found to be higher than the *lgs1* transcript levels in the control plants, suggesting that the mutation might disrupt the pairing of the *LGS1* mRNA with miR396. In addition to producing larger grains, *LGS1* also enhanced cold tolerance at the seedling stage and increased the survival rate of seedlings after cold stress treatment. These findings indicate that the mutation in *LGS1* appears to disturb the *GRF4*–miR396 stress response network and results in the development of enlarged grains and enhancement of cold tolerance in rice.

**Keywords:** Cold tolerance, grain size, map-based gene cloning, microRNA, OsGRF4, RNA sequencing.

## Introduction

Rice (*Oryza sativa* L.) can grow in a wide range of environments, and provides the main calorific intake for more than half of the world's population (Huang *et al.*, 2013). As the world's population is predicted to reach 9 billion by the middle of this century, requiring a 70–100% increase in food production relative to the current levels (Godfray *et al.*, 2010; Abe *et al.*, 2012), it is a great challenge to ensure sustainable food production and supplies worldwide. Among the yield-associated traits, the thousand-grain weight is restricted mainly by the grain shape, which can be further characterized by the grain length, grain width, and grain thickness. In addition, rice grain shape is known to strongly affect grain yield, grain quality, and market values (Huang *et al.*, 2013; S. Wang *et al.*, 2015). Thus, grain shape is an important trait in rice breeding programs.

More than 400 quantitative trait loci (QTLs) associated with the rice grain shape trait have been identified, and nearly 30 genes have been cloned and demonstrated to regulate the traits of grain shape and grain weight in various genetic studies (Huang *et al.*, 2011, 2013; Zhao *et al.*, 2011; Liu *et al.*, 2015; S. Wang *et al.*, 2015; Y. Wang *et al.*, 2015; Wu *et al.*, 2017). The identification and functional characterization of these genes have provided an important theoretical basis for the enrichment of genetic resources and development of new breeding and cultivation strategies in rice.

Growth-regulating factors (GRFs) are a family of plant-specific proteins that regulate the size and number of tissues, organs, and cells in plants (Van der Knapp *et al.*, 2000). GRFs contain two highly conserved regions, the QLQ (Gln, Leu, Gln) and the WRC (Trp, Arg, Cys) domains, both of which are present in the N-terminal regions of the protein (Van der Knapp *et al.*, 2000; Kim *et al.*, 2003; Choi *et al.*, 2004; Jones-Rhoades and Bartel, 2004; Kim and Kende, 2004; Zhang *et al.*, 2008; Kim *et al.*, 2012). The expression of GRFs is regulated at the transcriptional level by endogenous miRNAs, which base-pair with the corresponding region of mRNA coding for the WRC domain, resulting in target mRNA cleavage (Jones-Rhoades and Bartel, 2004; Jones-Rhoades *et al.*, 2006; Gao *et al.*, 2010; Liu *et al.*, 2014; Duan *et al.*, 2015; Hu *et al.*, 2015; Li *et al.*, 2016).

In this study, we took the map-based approach to clone a semi-dominant grain shape locus, designated as *Large Grain Size 1* (*LGS1*). *LGS1* encodes a GRF4 transcription factor and contains a 2 bp missense mutation corresponding to the WRC domain. The identification of *LGS1* will greatly facilitate the improvement of grain shape in rice through molecular marker-assisted selection approaches.

## Materials and methods

### Identification of LGS1

The mutant line JF178 (*Oryza sativa* L. ssp. *indica* cv) that produced larger and longer grains (Fig. 1A–E; Supplementary Table S2 at *JXB* online) was selected from the progeny of the rice cultivar Ma85 (*O. sativa* L. ssp. *indica* cv) that was subjected to mutagenesis by γ-Co$^{60}$ irradiation in the 1990s. JF178 and Samba (*O. sativa* L. ssp. *japonica* cv) were chosen as parents for mapping QTLs for grain length (Fig. 1F; Supplementary Fig. S1). A set of *LGS1* near-isogenic lines (NILs) was developed by crossing the small grain cultivar Samba (maternal parent) with JF178 (paternal parent). $F_1$ plants that contained the *LGS1* locus as identified through marker-assisted selection were chosen for backcross using Samba as the recurrent parent. NIL-*LGS1*$^{JF178}$ was finally selected from the $BC_{10}F_3$ generation in the Samba genetic background (Supplementary Fig. S1). For phylogenetic tree analysis of *LGS1*, a total of 47 rice cultivars collected in China and the JF series of breeding lines from our research group were used for PCR amplification utilizing the marker-assisted selection primers and *LGS1* PCR primers (Supplementary Tables S1, S2).

### Growing conditions and traits measurement

Rice plants were cultivated twice a year in the experimental field of Xiamen University, Fujian Province, China, and were planted with an interplant spacing of 20×20 cm$^2$ for transplanting. The plants were arranged in a completely randomized block design with three repeats. The traits of thousand-grain weight, grain length, grain width, grain number per panicle, plant height, spike length of the main stem panicle, and of the primary, secondary, and tertiary branch panicles were measured using 30 plants. Fully filled grains were chosen for measurement at the harvest stage. Grain yield per unit area was measured from 100 plants for each variety.

### Tissue section and microscopy

Rice spikelets were sampled at the heading stage and fixed in the formalin–acetic acid–alcohol (FAA) solution (5% formaldehyde, 5% glacial acetic acid, and 50% ethanol), followed by degassing under a vacuum pump for 25 min, and incubation in the FAA solution for at least 24 h. Fixed tissue samples were dehydrated in an ethanol solution series, destained in xylene solution, and embedded in paraffin. Tissue sections (7 μm thick) were cut with a rotary microtome (Leica, Germany) and mounted on a glass slide, followed by treatment with xylene and staining with 0.2% toluidine blue (Sigma, Germany). Sections were photographed under a Nikon 50i microscope (Nikon, Japan).

### Scanning electron microscopy

The entire spikelet hulls and endosperm were collected at the harvest stage and used for SEM. Gold-plated outer surface cells of the lemma and palea from mature seeds and endosperm slices (2 mm thick) were observed under a JSM-6390LV scanning electron microscope (JEOL, Japan) at 5 kV. The cell length and width, and the endosperm cell number per unit area were measured using Image IS Capture software (TuSimple, China). The cell number along both the longitudinal axis and transverse axis was recorded.

### Plasmid construction and genetic transformation

For construction of p*LGS1::LGS1* for genetic complementation (Supplementary Fig. S3A), a DNA fragment of 7.4 kb containing the 2.7 kb promoter, the 3.825 kb coding region, and the 0.9 kb termination site was amplified from Ma85 and JF178, and cloned into binary vector pCAMBIA1301. The resulting vectors, *plgs1*$^{Ma85}$*::lgs1*$^{Ma85}$ and *pLGS1*$^{JF178}$*::LGS1*$^{JF178}$, were introduced into JF178 and Ma85, respectively.

To construct the *LGS1* RNAi plasmid, two DNA fragments unique to *LGS1* [a 194 bp fragment containing the 84 bp 5'-untranslated region (UTR) and the other fragment 110 bp downstream from the *LGS1* start codon; Supplementary Fig. S3B] were amplified from JF178 and Samba, and cloned into pCUbi1390 (Okuley *et al.*, 1994; Smith *et al.*, 2000; Wesley *et al.*, 2001; Stoutjesdijk *et al.*, 2002). The expression of the *LGS1* RNAi was driven by the ubiquitin promoter. The resulting *LGS1*$^{JF178}$ and *lgs1*$^{Samba}$ RNAi vectors were introduced into JF178 and Samba, respectively.

The *lgs1* promoter::GUS (β-glucuronidase) reporter plasmid (Supplementary Fig. S3C) was constructed by fusion of the 2.8 kb *lgs1* promoter (including 36 bp downstream from the *lgs1* start codon) from Ma85 to the *GUS* reporter gene. The construct was subcloned into pCAMBIA1381Xa to generate *plgs1::GUS*, which was used to transform the rice cultivar Zhonghua 11 (*O. sativa* L. ssp. *japonica* cv).

Plasmids were confirmed by DNA sequencing and introduced into *Agrobacterium tumefaciens* strain EHA105 for rice transformation as described previously (Hiei *et al.*, 1994). Positive transgenic plants of the $T_2$ generation were used for recording of grain shape data.

### Histochemical GUS assays

Specimens were stained for GUS activity as described by Jefferson *et al.* (1987), and photographed under a BX50 OLYPUS microscope (Olympus, Japan).

### Quantitative RT–PCR of mRNA, and miRNA analysis

Total RNA and miRNA were extracted from various rice tissues using the Wolact® Plant RNA Isolation Kit (Wolact, Hong Kong, China). cDNAs were reverse transcribed using the RevertAid First Strand cDNA Synthesis Kit (Thermo Fisher Scientific, Waltham, MA,
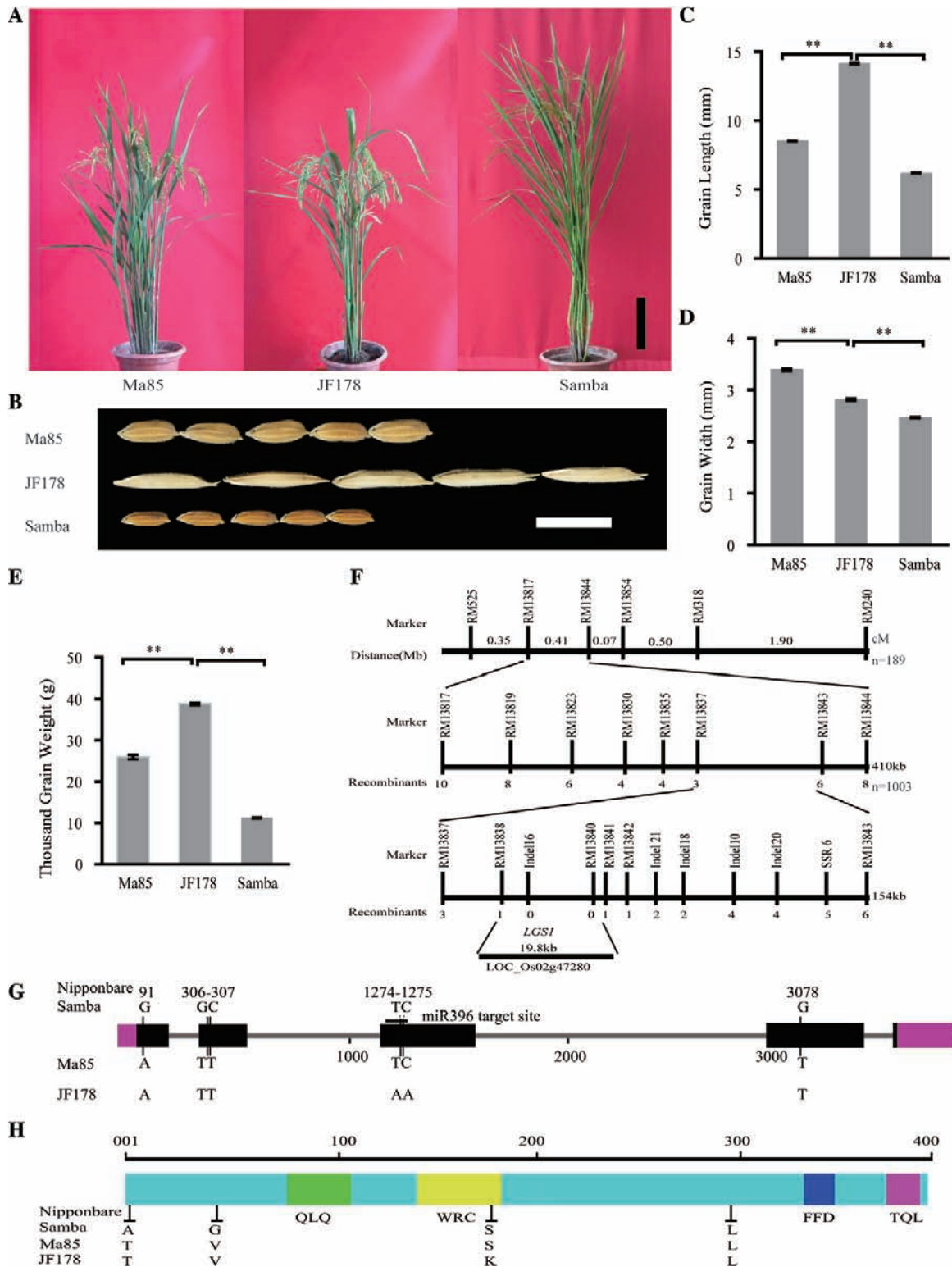
**Fig. 1.** Map-based cloning of *LGS1*. (A) Plant phenotype of Ma85, JF178, and Samba. Scale bar=20 cm. (B) Grain phenotype of Ma85, JF178, and Samba (*n*=5). Scale bar=10 mm. (C–E) Comparisons of grain length (C), grain width (D), and thousand-grain weight (E) among Ma85, JF178, and Samba (*n*=90). Values are given as the mean ±SE. **P<0.01, Student's *t*-test. (F) Fine mapping of *LGS1*. The numbers under each marker indicate the number of recombinants between *LGS1* and the molecular markers. (G) Gene structure and sequence variations of LGS1 among JF178, Ma85, Samba, and Nipponbare. The blocks represent exons, and the 5'- and 3'-UTRs, the lines represent introns, and the vertical lines indicate the nucleotide sequence variations in exons. (H) Domain structure of LGS1 protein and amino acid variations among JF178, Ma85, Samba, and Nipponbare. The blocks indicate different conserved domains. The vertical lines indicate amino acid variations. (This figure is available in colour at *JXB* online.)

USA). miRNAs were reverse transcribed using the Taqman® miRNA Reverse Transcriptase Kit (Thermo Fisher Scientific, Foster, CA, USA) and stem–loop reverse transcription primers (Sangon, Shanghai, China).

Quantitative RT–PCR was carried out using TransStart Top Green qPCR SuperMix (Transgene Biotech, Beijing, China) with *OsActin1* (for mRNA) or the U6 (for miRNA) gene as an endogenous control for fold

enrichment. Quantitative RT–PCRs of mRNA and miRNA analyses were carried out using the CFX96 Real-Time PCR System (Agilent, California, USA) in accordance with the manufacturer's instructions. The qPCR cycling conditions were 2 min at 95 °C followed by 38 cycles of amplification (95 °C for 15 s, 60 °C for 20 s, and 72 °C for 25 s). All assays were repeated at least three times using independent RNA samples and performed with three technical repetitions. The sequences of primers are given in Supplementary Table S1.

### Subcellular localization

For subcellular localization experiments (Supplementary Fig. S3D; Supplementary Table S1), the coding sequence of *LGS1* was amplified from JF178, and inserted into pDONR201-GFP-LGS1. The plasmid was used to react with pK2GW7 (Invitrogen, Carlsbad, CA, USA) to generate *PCAMV35S::GFP-LGS1*. The vector was introduced into *A. tumefaciens* strain GV1301 for transformation into *Arabidopsis thaliana*. *PCAMV35S::Collin-RFP* was used as a nuclear localization marker (Cui *et al.*, 2015). All Arabidopsis plants were grown in soil at 22 °C under long days (16 h light/8 h dark) with white fluorescent light (120 μmol m$^{-2}$ s$^{-1}$). Green and red fluorescence signals of 2-week-old transgenic plants were observed under a confocal laser scanning microscope (Zeiss LSM 780/ Carl Zeiss Meditec AG, Jena, Germany).

### Transactivation activity assays in yeast

Various segments of *LGS1* with truncated cDNA were amplified from JF178 and Ma85, and cloned into the pGBKT7 vector for transcriptional activation activity analysis by the yeast two-hybrid system according to the manufacturer's protocol (Clontech, USA). The empty pGBKT7 vector was used as control. The prey and bait plasmids were co-transformed into the yeast Y2H Gold strain, which was grown in SC/DDO-Trp/-Leu (synthetic complete medium with dropout of Trp and Leu), SC/DDO-Trp/-Leu+100 ng ml$^{-1}$ Aureobasidin A (AbA) medium for 2 d at 30 °C. The interactions between GRF and GIF (GRF-interacting factor) were assayed in the Matchmaker GAL4 Two-Hybrid System (Clontech, USA). LGS1$^{JF178}$ and lgs1$^{Ma85}$ proteins were expressed as bait from pGBKT7. The coding sequences of OsGIF1, OsGIF2, and OsGIF3 were amplified from Ma85 and expressed as prey from pGADT7. The interaction assays were based on the growth ability of the co-transformants on medium supplemented with AbA. The experiments were repeated three times.

### RNA-seq and data analysis

Tissue samples of 5–6 cm long young panicles, corresponding to the differentiation stage of meiotic division of pollen mother cells, were taken from rice plants grown under field conditions, and collected for total RNA extraction. To obtain a comprehensive profile of the *LGS1* transcriptome, library construction was performed with a NEBNext® Multiplex RNA Library Prep Set (NEB), which used the Illumina Hiseq 2000 to perform high-throughput RNA sequencing (RNA-seq) of the recurrent parent (Samba) and the NIL line (NIL-*LGS1*$^{JF178}$). In total, 30.68 Gb of clean RNA-seq reads were generated from the six libraries, and mapped to the rice genome using TopHat2 (Trapnell *et al.*, 2010; Kim *et al.*, 2013). The transcriptome data were collected from three replicas of the wild-type control and three replicas of the *LGS1* NIL line. The number of fragments per kilobase of transcript per million mapped reads (FPKM) was analyzed for gene expression. Differentially expressed genes (DEGs) were defined by a 2-fold change expression difference at a false discovery rate (FDR) of <0.01. The genome data of Nipponbare (*O. sativa* L. ssp. *japonica* cv) were used as a reference.

### Abiotic stress treatment and cold treatment

NIL-*LGS1*$^{JF178}$ and Samba were used for analysis of the response to plant hormone treatment. Ma85 and JF178 were used for stress treatment. Rice seeds were germinated and seedlings were grown for 15 d under normal growth conditions (14 h light, 28 °C/10 h dark, 20 °C, 20000LX; Yiheng,

Shanghai, China) with daily watering. Seedlings were then treated for 12 h with normal growth conditions (the control), 35 °C, 4 °C, 20 mg ml$^{-1}$ GA$_3$ (gibberellic acid 3), 1 mg ml$^{-1}$ IAA (indole-3-acetic acid), 25 mg ml$^{-1}$ ABA (abscisic acid), 20 mg ml$^{-1}$ BL (brassinolide), 0.25 g ml$^{-1}$ NaCl, and 0.1 g ml$^{-1}$ NaHCO$_3$ (pH 9.0), or UV-B (TL20W/01RS; Philips, Eindhoven, The Netherlands) for 1 h. Seedlings were then sampled for quantitative real-time PCR (qRT-PCR) analysis of *LGS1* expression.

For cold stress treatment, 15-day-old seedlings were held at 4 °C for different periods of time as indicated, and then sampled for qRT-PCR analysis. After the cold treatment, seedlings were grown under normal growth conditions for 5 d to recover from the cold stress. The survival rates after the recovery from cold treatment were recorded, and the seedlings were sampled for qRT-PCR analysis of expression of *lgs1* and miR396.

### Accession codes

Accession codes for the DNA Data Bank of Japan (DDBJ) are as follows: LGS1_JF178, LC333009; lgs1_Ma85, LC333010; and lgs1_Samba, LC333011.

## Results

### Mapping of LGS1 and polymorphisms in rice germplasm

JF178 and Samba were selected as parents to map QTLs for grain length. JF178 is a larger grain *indica* mutant line (thousand-grain weight, 39.0±0.6 g; grain length, 14.16±0.05 mm), whereas Samba is a small grain *japonica* variety (thousand-grain weight, 11.9±0.1 g; grain length, 6.21±0.02 mm; Fig. 1A–E). Using 189 random subpopulations of the BC$_5$F$_2$ segregating population, we were able to perform primary mapping of *LGS1*, the major QTL locus affecting grain shape in JF178, to a region between markers RM13817 and RM13844 on chromosome 2 (Supplementary Fig. S1A). Using 1003 recessive plants (short grain, grain length <6.2 mm) from the BC$_5$F$_3$ population, we fine-mapped *LGS1* to a 154 kb interval between markers RM13838 and RM13841 on chromosome 2 (Supplementary Fig. S1A, B). From the 1003 recessive plants of the BC$_5$F$_3$ population, we identified 18 recombinant plants, which allowed us to narrow down the *LGS1* locus to a 19.8 kb region between markers RM13838 and RM13840 on the long arm of chromosome 2 (Fig. 1F; Supplementary Fig. S1A, B). This region contains only one gene, LOC_Os02g47280, the only candidate for *LGS1* (Fig. 1F). Comparison between the genomic DNA and cDNA sequences of *LGS1* revealed the presence of five exons and four introns for *LGS1*, with the full-length DNA of 3825 bp encoding 394 amino acids (Fig. 1G, H). Comparison of the nucleotide sequences of *LGS1* alleles from Ma85 and JF178 revealed two nucleotide substitutions (TC to AA) in exon 3 that resulted in the amino acid substitution of serine to lysine (S163K) in the LGS1 protein (Fig. 1G, H; Supplementary Table S2). We then analyzed the nucleotide sequences of *LGS1* from the irradiated mutant lines of our collection and the natural germplasm resources. Multiple polymorphisms in the *LGS1* coding region and non-coding region were detected. These polymorphisms can be grouped into three types: haplotype I (two nucleotide substitutions), haplotype II (natural nucleotide sequence of *indica* subspecies), and haplotype III (natural nucleotide sequence of *japonica*

subspecies). There are three single nucleotide polymorphisms (SNPs) between haplotype II and III. SNP1 has a one nucleotide difference, resulting in an amino acid change to T2A in the *japonica* subspecies. SNP2 contains a variation of two nucleotides, resulting in an amino acid change to V41G in the *japonica* subspecies. SNP3 has a one nucleotide difference that does not alter the amino acid residue between *indica* and *japonica* subspecies (Fig. 1G, H; Supplementary Tables S2, S3). These data indicate that the two nucleotide substitution at position 477–488 of *LGS1* is the cause of the large grain shape trait observed in JF178 and other mutant lines from our experimental station.

### LGS1 is a semi-dominant gene regulating grain shape and panicle traits

We performed reciprocal crosses of JF178 and Samba, and assayed the grain traits of F$_1$ plants. Our data showed that there was no significant difference between the reciprocal crosses in grain length, grain width, thousand-grain weight, grain thickness, and grain number of the main panicle (Supplementary Fig. S2A–F), suggesting that *LGS1* is a typical nuclear inherited locus with no maternal effect on grain traits. Analysis of grain trait data showed that grains of the homozygous and heterozygous NILs (NIL-*LGS1*$^{JF178}$ and NIL-*LGS1*$^{JF178}$/*lgs1*$^{Samba}$) were 20.47% and 13.83% longer, 14.95% and 11.35% wider, and 42.81% and 28.53% heavier, respectively, than those of Samba (Fig. 2A–E; Supplementary Fig. S1). This finding suggests that *LGS1* regulates grain length, grain width, and thousand-grain weight in rice. The grain filling rate was also greatly increased in NIL-*LGS1*$^{JF178}$ as compared with Samba (Fig. 2G, I, J), resulting in a significant increase (15.72%) in grain yield in NIL-*LGS1*$^{JF178}$ (Fig. 2H). In addition, analysis of plant height and panicle traits in NILs revealed that *LGS1* had pleiotropic effects on the spike length, effective panicles (tillers), and tertiary branches per panicle (Fig. 2F; Supplementary Fig. S2G–L). Taken together, these analyses suggest that *LGS1* is a semi-dominant gene with pleiotropic effects on grain shape and panicle traits in rice.

To verify the *LGS1* function on grain traits, we introduced the *pLGS1::LGS1* vector (Supplementary Fig. S3A) containing the *LGS1* allele from JF178 into the small-grain cultivar Ma85. Transgenic plants were found to have increased transcript levels of *LGS1* at the young spike differentiation stage, the critical time of reproductive development in rice. We selected four transgenic lines expressing the *LGS1* allele and compared them with Ma85. Grains produced by the four transgenic lines (MaCP01–MaCP04) were longer (6.75, 5.31, 10.02, and 37.08%, respectively), wider (1.89, 3.05, 4.79, and 19.34%), and heavier (6.96, 15.66, 21.33, and 33.93%) than those of the control Ma85 (Fig. 3A, D; Supplementary Fig. S4A–C). We also performed the reciprocal experiment by introducing the *plgs1::lgs1* vector (Supplementary Fig. S3A) containing the Ma85 allele into JF178. Transgenic plants of JF178 expressing the Ma85 *lgs1* allele did not change the transcript level of its native *LGS1* (Fig. 3E). Grains of the two transgenic lines (JFCP01 and JFCP02) were shorter (2.05% and 5.14% reduction, respectively), not significantly different in width (only 1.10% and 2.80% reduction in grain width),

and considerably lighter in thousand-grain weight (26.50% and 30.81% reduction) (Fig. 3B; Supplementary Fig. S4D–F). These results further suggest that *LGS1* is a semi-dominant gene with pleiotropic effects on multiple grain traits, which is consistent with the conclusion from genetic observations described above.

### LGS1 is highly expressed in young vegetative tissues and developing grains

To investigate the temporal and spatial expression patterns of *lgs1*, we constructed the *plgs1*$^{Ma85}$*::GUS* reporter vector (Supplementary Fig. S3C) and used it to transform Zhonghua 11. The GUS signals were considerably stronger in the growing tissues of root, internode, node, leaf, sheath, spike-stalk, pulvinus, ligule, and auricle than in the mature tissues (Fig. 4A). The GUS signal remained strong in the nodes of mature plants (Fig. 4A), where there was still active meristematic activity. During panicle development, the GUS activity was markedly stronger in the developing flowers, pistils, stamens, hulls, and fruits than in ripened grains (Fig. 4B, C; Supplementary Table S4).

### Transcript levels of LGS1 are higher in large grain NILs

We performed qRT-PCR to detect the expression of *LGS1* in NILs. Our results showed that the transcript levels of *LGS1* in the large grain NIL-*LGS1*$^{JF178}$ were significantly higher in roots, stems, leaves, young panicles (stages III–VI), and developing fruits (15, 21, and 27 d after fertilization) than those of the small grain Samba. The differences in transcript levels between NIL-*LGS1* and Samba were highly significant at stages IV–V (~5 cm young spikes) (Fig. 4D–F; Supplementary Table S4). Based on these observations, we conclude that *LGS1* is expressed widely in various developing tissues and organs in rice and that its expression levels positively correlate with grain size.

### Grain size is reduced in transgenic plants expressing LGS1 RNAi

To verify the hypothesis that the *LGS1* mRNA level correlated with its function in grain development, we constructed the ubiquitin promoter-driven RNAi vectors *pUbi::lgs1*$^{Samba}$ and *pUbi::LGS1*$^{JF178}$ (Supplementary Fig. S3B), and used them to transform Samba and JF178, respectively. The expression level of *LGS1* was found to be strongly reduced in young panicles of transgenic Samba and JF178 plants expressing the corresponding RNAi construct. As a result, grains of RNAi-expressing Samba and JF178 were not significantly different and there was a 4.75% reduction in grain length, 4.09% and 12.90% reductions in grain width, and 11.28% and 17.72% reductions in thousand-grain weight, respectively (Fig. 3C, F; Supplementary S4G–I). Taken together, these observations indicate that the *LGS1* allele from JF178 causes the *LGS1* mRNA to accumulate and increases grain length, grain width, and thousand-grain weight in JF178 mutant plants, NIL-*LGS1*$^{JF178}$ plants, and transgenic Ma85 plants expressing *LGS1*$^{JF178}$.
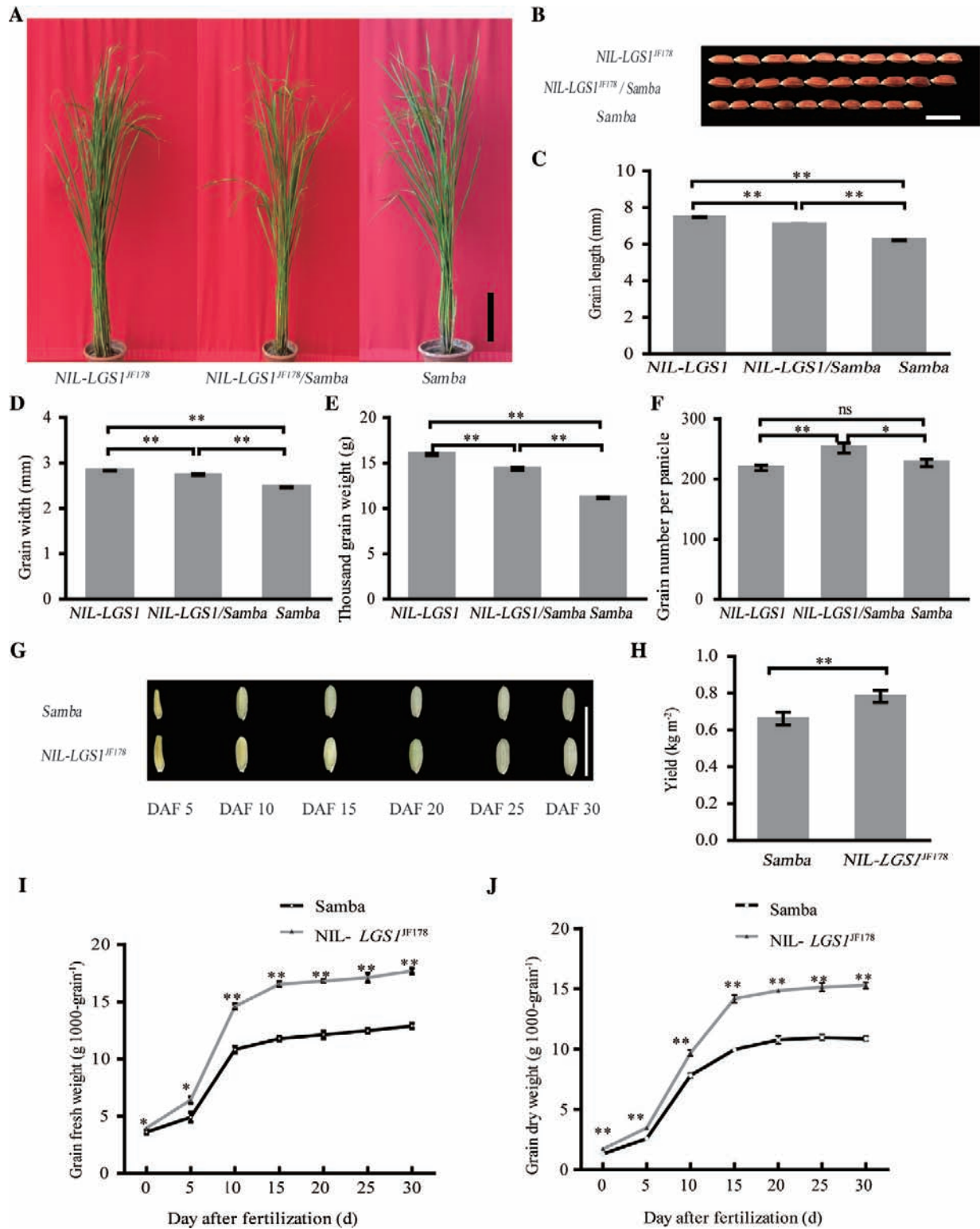
**Fig. 2.** Grain size phenotype of near-isogenic lines (NILs). (A) Morphological characteristics of *LGS1* NILs. Scale bar=20 cm. (B) Grain shape phenotype of *LGS1* NILs (*n*=10). Scale bar=10 mm. (C–F) Comparisons of grain length (C), grain width (D), thousand-grain weight (E), and grain number per panicle (F) in *LGS1* NILs (*n*=90–3000). (G) Characterization of grain filling in *LGS1* NILs (DAF, day after fertilization). Scale bar=10 mm. (H) Yield per unit area at the harvest stage (*n*=3). (I) Time-course of grain fresh weight increase (*n*=300). (J) Time-course of grain dry weight increase (*n*=300). *LGS1* from JF178 is a semi-dominant allele. NIL-*LGS1*$^{JF178}$ (NIL-*LGS1*) contains the *LGS1* allele from JF178 in the Samba genetic background. Samba carries the *lgs1* allele and serves as a control. Values are given as the mean ±SE. ns $P$>0.05, *$P$<0.05, **$P$<0.01 were calculated by Student's *t*-test. (This figure is available in colour at *JXB* online.)

### *LGS1 encodes rice growth-regulating factor 4*

The deduced peptide sequence of *LGS1* encodes the putative transcription factor OsGRF4 (rice growth-regulating factor 4; Fig. 1H), one of the 12 members of the GRF family. Similar to most other GRF proteins, LGS1 contains a QLQ domain that may be involved in chromatin remodeling, a WRC domain that may participate in transcription regulation, and
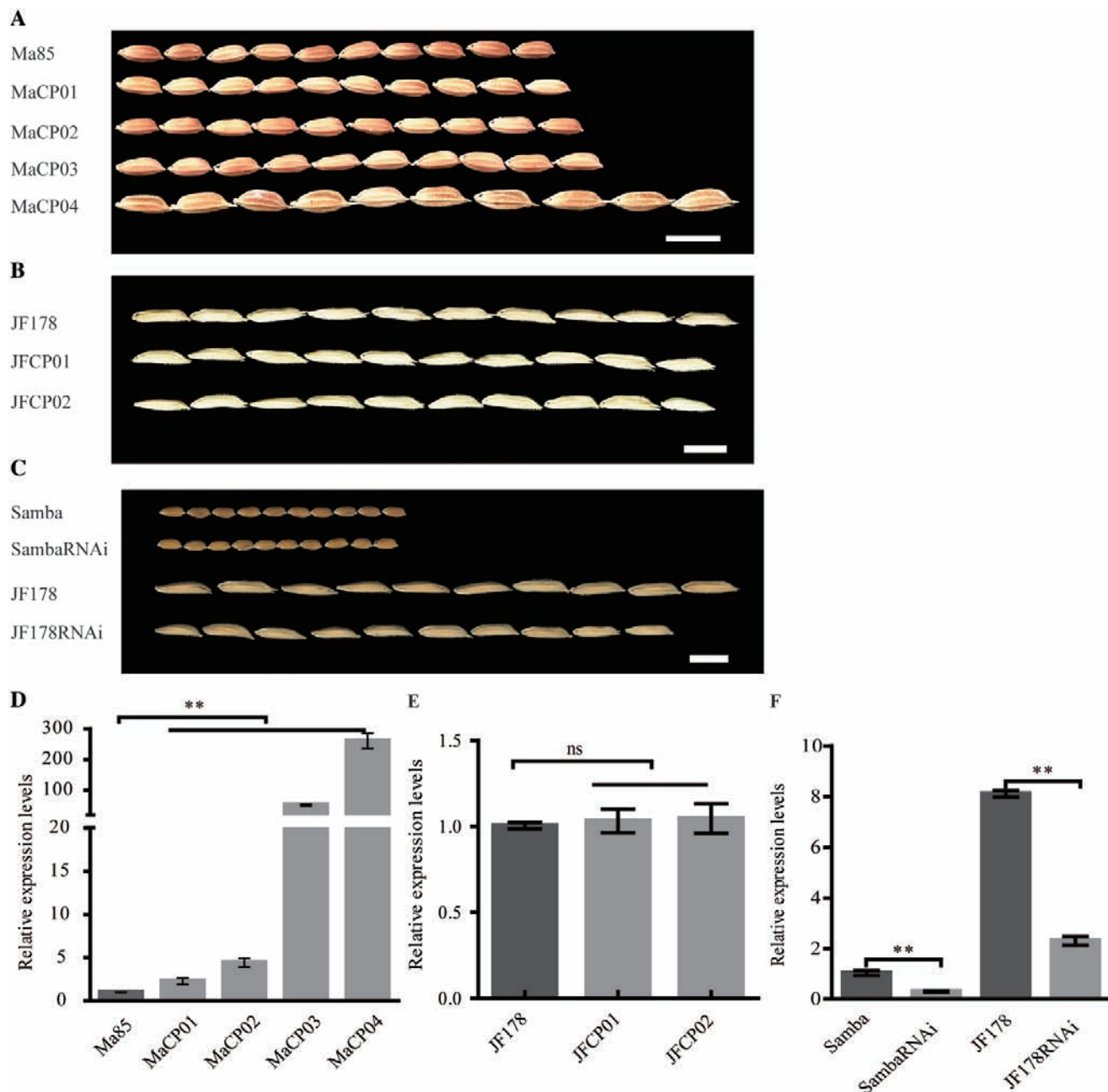
**Fig. 3.** Grain phenotype of transgenic plants and *LGS1*-RNAi plants. (A–C) Grain phenotype of Ma85 and four transgenic lines of Ma85 expressing the genetic complementation vector p*LGS1::LGS1* (A), JF178 and two lines of JF178 expressing *plgs1::lgs1* (B), and Samba and JF178 expressing the *LGS1*-RNAi construct (C). Scale bars=1 cm in (A–C). (D–F) Transcript levels of *LGS1* in Ma85 and four transgenic lines of Ma85 expressing p*LGS1::LGS1* (D), JF178 and two transgenic lines of JF178 expressing *plgs1::lgs1* (E), and Samba, JF178, and transgenic RNAi plants (F). RNA was isolated from young panicles (5 cm long, *n*=4). MaCP, transgenic Ma85 expressing the complementation vector p*LGS1::LGS1*; JFCP, transgenic JF178 expressing *plgs1::lgs1*. Ma85, JF178, and Samba and JF178 were used as controls in (A) and (D), (B) and (E), and (C) and (F), respectively. Values are given as the mean ±SE. ns *P*>0.05, **$P<0.01$ were calculated by Student's *t*-test. (This figure is available in colour at *JXB* online.)

two other domains (FFD and TQL) with unknown functions (Fig. 1H). The mutation in JF178 occurs in the WRC domain with a serine to lysine substitution at position 163 of LGS1 (Fig. 1H). The LGS1 protein was localized to the cell nucleus (Supplementary Fig. S3D, I), and had transcription activation activity when expressed in yeast cells (Supplementary Fig. S3E–G, J). Using the yeast one-hybrid system, we were able to further delimit the activation domain of LGS1 to its C-terminus (Supplementary Fig. S3E–G , J).

It has been reported that GRF proteins interact with GIF family members, and form GRF–GIF complexes in Arabidopsis, maize, and rice (Kim and Kende, 2004; Zhang *et al.*, 2008; Duan *et al.*, 2015; Kim and Tsukaya, 2015; Li *et al.*, 2016). To test if any GIF may interact with LGS1, we cloned OsGIF1 (Os11g0615200), OsGIF2 (Os12g0496900), and OsGIF3 (Os03g0733600), and expressed them as prey proteins in the yeast two-hybrid system (Supplementary Fig. S3E, H). LGS1^JF178 and lgs1^Ma85 were expressed as bait. The
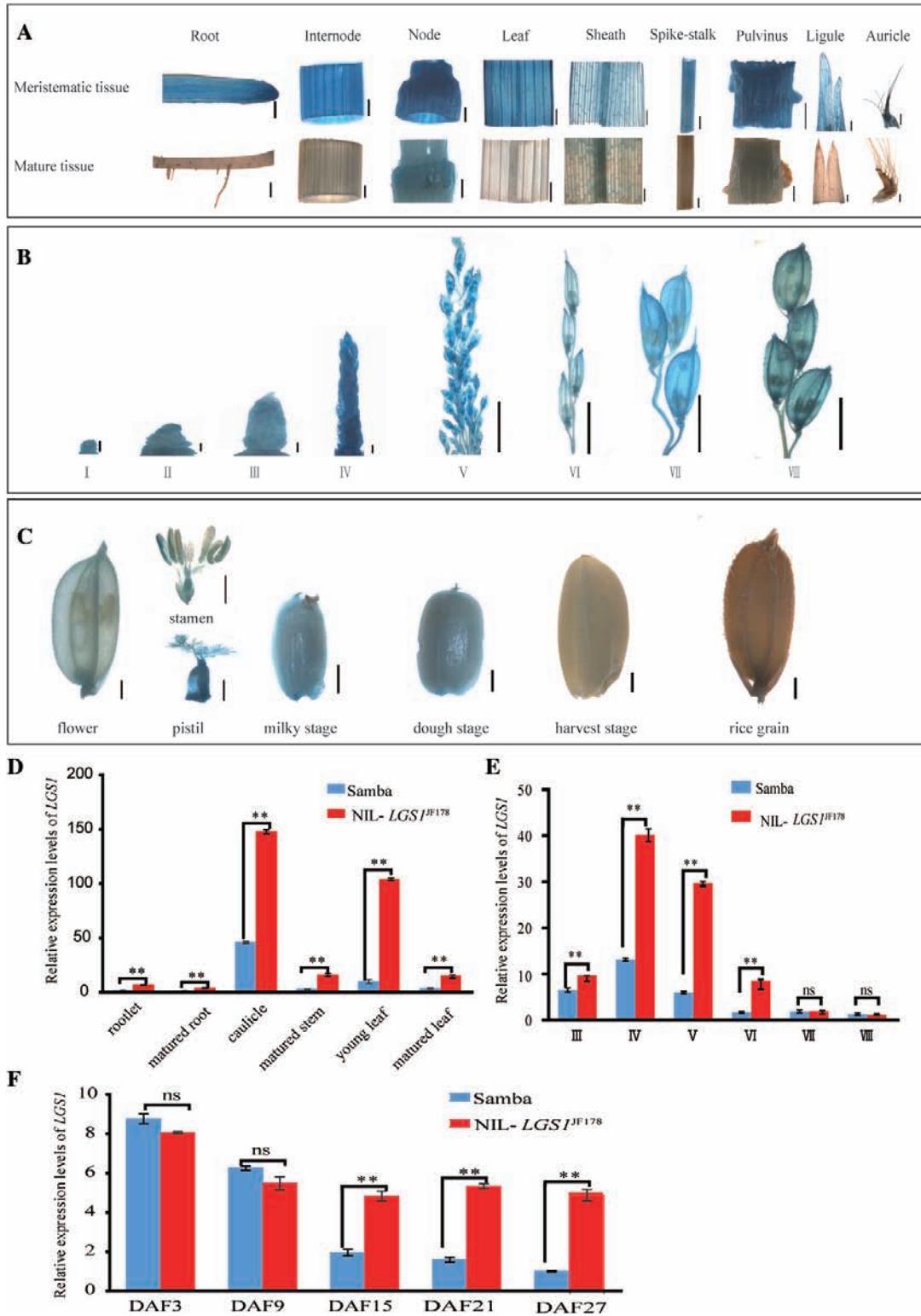
**Fig. 4.** Temporal and spatial expression patterns of *LGS1*. (A–C) Expression patterns of *LGS1* in vegetative tissues (A), panicle meristems and developing young panicles (B; Supplementary Table S4), and developing fruits (C). Scale bars=1 mm in (A) (root, internode, node, leaf, sheath, and spike-stalk) and (C); 100 µm in (A) (pulvinus and ligule); 500 µm in (A) (auricle) and (B) (I, II, III, IV), and 5 mm in (B) (V, VI, VII, VIII). (D–F) Relative expression levels of *LGS1* in vegetative tissues (D), developing young panicles (E), and developing fruits (F). DAF, day after fertilization. The expression levels of *LGS1* were measured by qRT-PCR (*n*=6). The expression values of mature leaves (D), stage VIII (E), and DAF 27 in Samba (F) are set as 1. Values are given as the mean ±SE. ns *P*>0.05, **P*<0.01 were calculated by Student's *t*-test. (This figure is available in colour at *JXB* online.)

results showed that both LGS1 and lgs1 (OsGRF4) inter-acted with the three OsGIFs tested. The interaction with OsGIF3 was stronger than that with OsGIF1 or OsGIF2 (Supplementary Fig. S3K). These results demonstrate that LGS1 interacts with OsGIFs and functions as a transcription factor.

*LGS1 controls grain size and milk filling rate*

Given that the NIL-*LGS1* spikelet hull was longer and wider than that of Samba at the flowering and harvest stages, we asked whether the increase in the hull size was caused by the increase in cell number, cell size, or both. We cut sections of paraffin-embedded spikelets and observed the longitudinal sections of the central spikelet hull, the surface sections of the lemma and palea, and cross-sections of endosperm under a scanning electron microscope (Fig. 5A–E). The length of lemma inner epidermal cells was significantly greater in NIL-*LGS1*[JF178] than in Samba (Fig. 5A, B). Specifically, the epidermal cells of the lemma and palea in NIL-*LGS1*[JF178] were longer (12.20% and 7.19% increase, respectively) and wider (5.44% and 16.44% increase, respectively) than those of Samba. Interestingly, there was also a significant increase in the longitudinal cell number of the lemma and palea (15.03% and 13.10% increase, respectively) in NIL-*LGS1*[JF178] compared with that in Samba. The transverse cell numbers of lemma and palea in NIL-*LGS1*[JF178] were not significantly different from those in Samba (Fig.

5C–I; Supplementary S5A–D). There was also no significant difference in endosperm cell size between NIL-*LGS1*[JF178] and Samba (Fig. 5E; Supplementary Fig. S5E). However, NIL-*LGS1* and Samba differed significantly in endosperm dry weight (Supplementary Fig. S5F), which resulted from the increased endosperm cell number and increased grain filling rate. Thus, our data demonstrate a significant increase in grain length, grain width, longitudinal cell number, and endosperm cell number in NIL-*LGS1*[JF178], thereby suggesting that *LGS1* may play a role in the regulation of cell division during grain development in rice.

*LGS1 regulates cell division and hormone response pathways*

To identify genes that are regulated by *LGS1*, we performed RNA-seq analyses in young panicles (~4–5 cm long, Fig. 6A) and compared the whole transcriptome profiles between NIL-*LGS1*[JF178] and Samba. A total of 1094 DEGs (ratio ≥2) were identified in the young panicles, among which 306 genes were
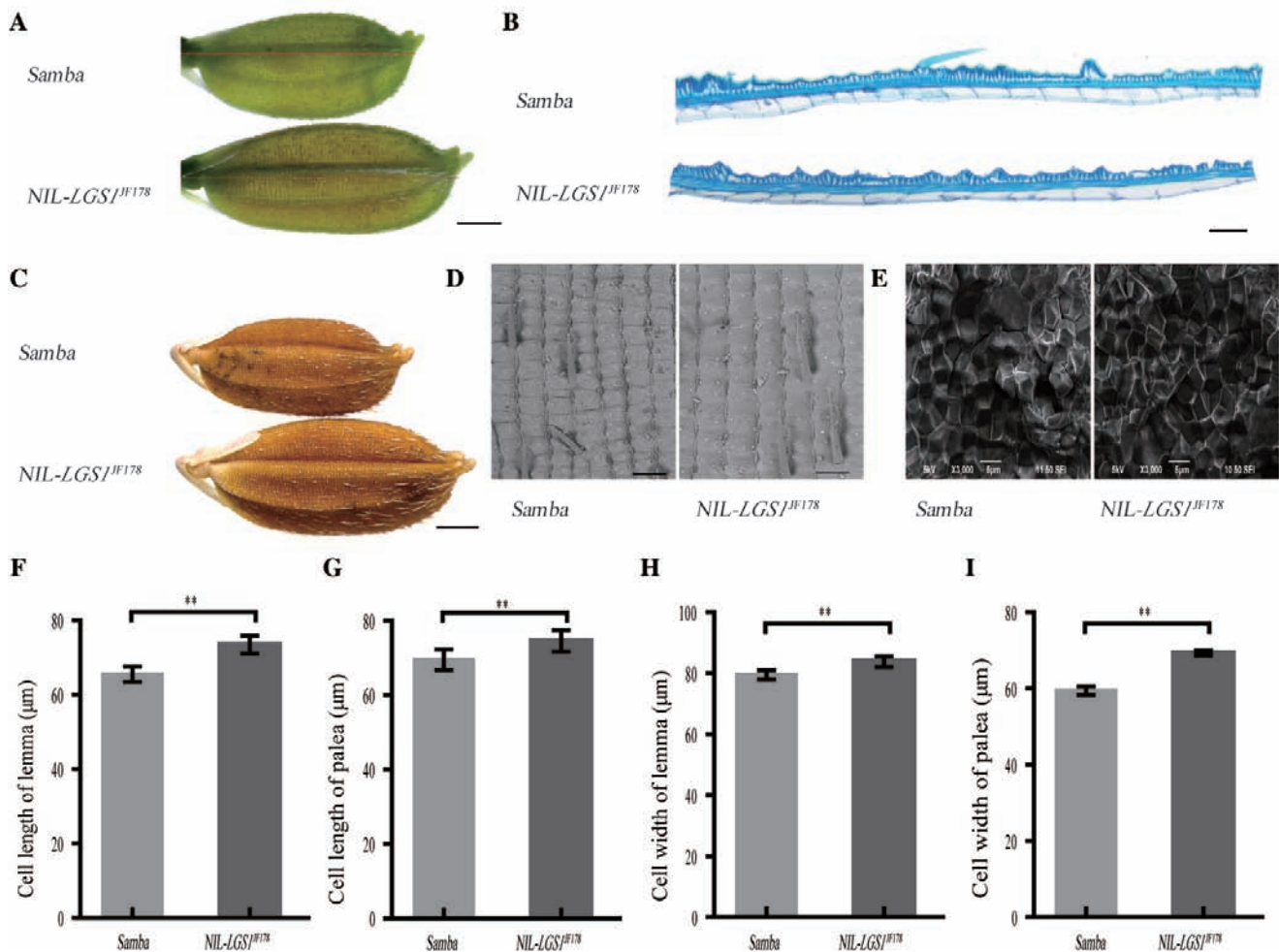


**Fig. 5.** Anatomic analyses of spikelet hulls at the heading stage and endosperm at the harvest stage in *LGS1*-NILs. (A) Spikelets. Scale bar=1 mm. The line indicates the position of the longitudinal section. (B) Magnified view of the spikelet hull longitudinal section of the lemma. Scale bar=100 μm. (C) Grain phenotype at the harvest stage. Scale bar=1 mm. (D) SEM analysis of the lemma surface in NILs. Scale bar=100 μm. (E) SEM analysis of the endosperm cross-section at the centre of the grain. Scale bar=5 μm. (F–I) Comparison of cell length of the lemma (F) and palea (G), and cell width of the lemma (H) and palea (I) in NILs (*n*=100). Samba as a control. Values are given as the mean ±SE. **\**P*<0.01 was calculated by Student's *t*-test. (This figure is available in colour at *JXB* online.)

up-regulated and 788 down-regulated (Fig. 6B). This observation indicates that the number of down-regulated genes was ~2.57 times that of the up-regulated genes (Fig. 6B). Enrichment analysis of function classification of clusters of

orthologous groups (COGs) identified the 'cell cycle control, cell division, chromosome partitioning' (2.96%) and 'signal transduction mechanisms' (6.61%) as the annotated DEG pathways (Fig. 6C). These analyses infer that *LGS1* may control
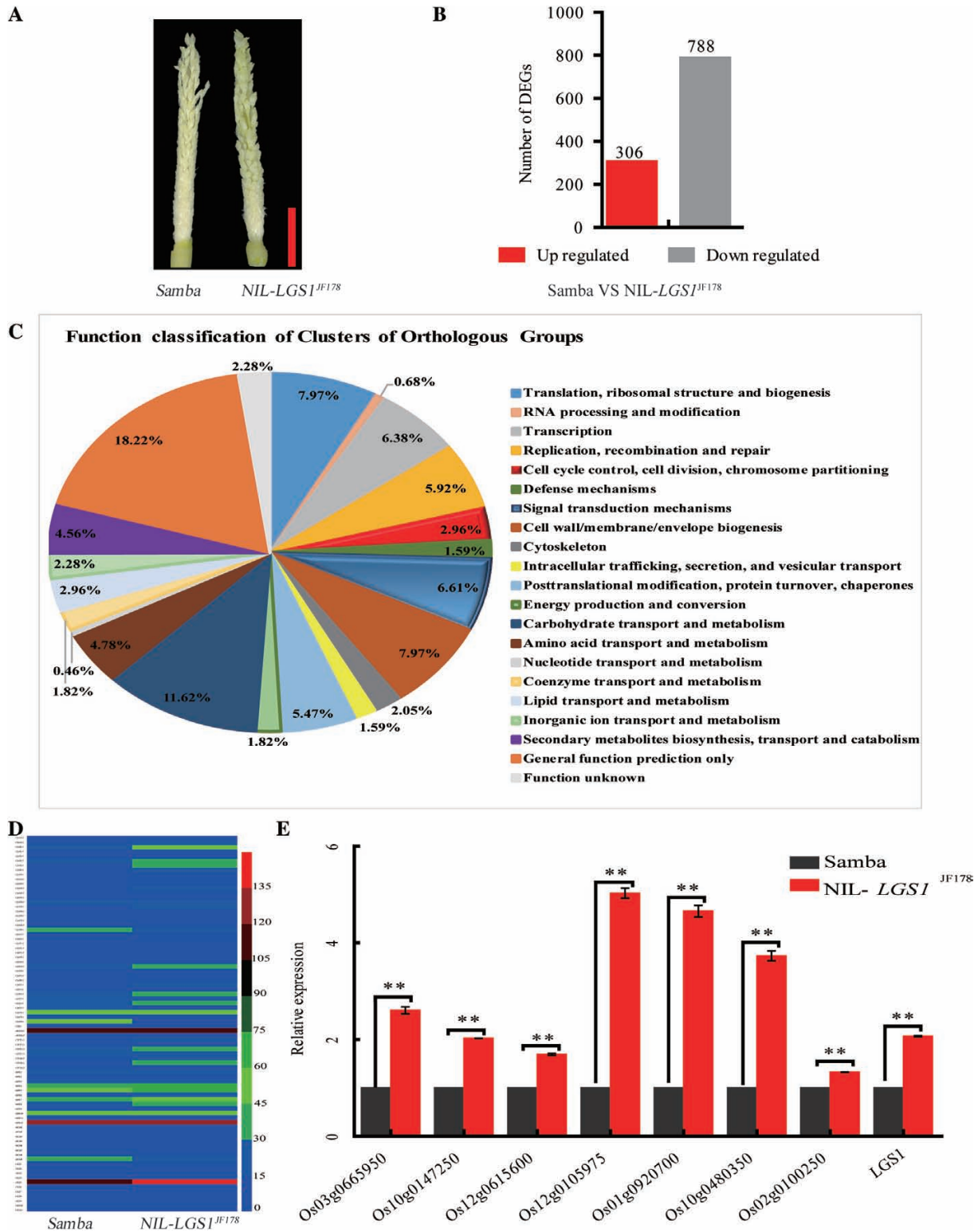


**Fig. 6.** RNA-seq analysis of *LGS1*-NILs. (A) Phenotype of young panicles. Scale bar=1 cm. (B) Number of differentially expressed genes (DEGs, >2-fold change) of NIL-*LGS1*[JF178] as compared with Samba. (C) DEG analysis of COG annotation. (D) Heat map of cell cycle-related DEGs (*n*=3). The scale bar, horizontal bars, and numbers indicate the FPKM (fragments per kilobase million) values. (E) Expression of the uncharacterized cell cycle-related genes by qRT-PCR (*n*=3). Samba as a control. Values are given as the mean ±SE. **$P<0.01$ was calculated by Student's *t*-test. (This figure is available in colour at *JXB* online.)

grain development through regulation of cell division, and participate in hormone responses.

We analyzed the 82 identified cell cycle genes that may affect the grain size (Fig. 6D; Supplementary Table S5). Analysis of annotated DEGs revealed that 25 DEGs encode cell cycle proteins, among which 11 were up-regulated and 14 down-regulated. Five DEGs encode expansin-like proteins, all of which were down-regulated. Nineteen DEGs encode leucine-rich repeat extensin-like proteins, among which seven were up-regulated and 12 down-regulated (Supplementary Table S6). We performed qRT-PCR to verify the up-regulated cell cycle genes (fold change >2) in NIL-*LGS1*[JF178], and our results confirmed that the expression levels of all genes tested were significantly higher in NIL-*LGS1*[JF178] than in Samba (Fig. 6E). These results demonstrate that *LGS1* may alter the expression of cell cycle genes to promote cell division, extension, and expansion, resulting in increased grain size.

We also noticed that there were significant increases in seedling fresh weight, dry weight, and seedling length in NIL-*LGS1*[JF178] as compared with Samba, whereas no significant difference in plant height at the harvest stage was observed between NIL-*LGS1* and Samba (Supplementary Figs S2G, S6A–H). These features indicate that *LGS1* may be involved in the hormone response pathways, which is consistent with the detection of DEGs in signal transduction pathways revealed by RNA-seq analysis (Fig. 6C). To explore this possibility, we treated NILs with different plant hormones (BL, ABA, IAA, and GA₃) and measured seedling length and lamina inclination. We observed that there were significant increases in seedling length in NIL-*LGS1*[JF178] in response to BL, ABA, and IAA as compared with the seedling length in Samba. The sensitivity of lamina inclination to BL treatment was impaired in NIL-*LGS1*[JF178], and no significant change in seedling height was observed in NIL-*LGS1*[JF178] treated with GA₃ as compared with that in Samba (Supplementary Fig. S7A–H). In summary, these crosstalk responses of plant hormones imply that *LGS1* may promote the growth of vegetative organs, resulting in more efficient nutrient supply for the later development of spikelets and endosperm. Whether and how the plant hormone signaling pathways are linked to the increased grain size in NIL-*LGS1*[JF178] remains to be studied in the future.

### *LGS1 transcript levels are regulated by miR396*

It has been documented that the *GRF* genes are targets of miRNA 396 (miR396), contain the miR396 recognition sequence in Arabidopsis, tobacco, and rice (Lan *et al.*, 2012; Baucher *et al.*, 2013; Liang *et al.*, 2014; Rodriguez *et al.*, 2015), and are responsive to stress (Gao *et al.*, 2010). Nine miRNA precursor sequences of the miR396 family in rice (*osa-miR396a–osa-miR396i*) were predicted from the miRbase and psRNA target databases (Supplementary Fig. S8A; Supplementary Table S7). Sequence analysis showed that the mutation site occurred within the complementary sequence of OsmiR396 (Fig. 1G). We investigated whether OsmiR396 plays a role in regulating the *LGS1* mRNA level

in rice. qRT-PCR analysis of young panicles revealed that the expression pattern of *lgs1* was opposite to that of OsmiR396; that is, the decrease in the *LGS1* mRNA level during stages IV–VIII coincided with the increase in the expression levels of OsmiR396 members (Supplementary Fig. S8B). These results suggest that the transcript abundance of *lgs1* is severely altered by *osa-miR396a–osa-miR396i* and further demonstrate that the expression of miR396 members down-regulates the transcript levels of *lgs1*.

### *LGS1 enhances cold tolerance at the seedling stage*

To investigate the role of *miR396a– osa-miR396i* in the regulation of *LGS1* during stress, we grew Ma85 and JF178 plants under different abiotic stress conditions or treated them with plant hormones. We found that *LGS1* expression was up-regulated by treatment with IAA and NaHCO₃, and slightly down-regulated by treatment with cold (4 °C), UV, ABA, and NaCl in JF178 as compared with the *lgs1* levels in Ma85. It was striking to note that *LGS1* expression was severely down-regulated by treatment with GA₃ and BL in JF178 as compared with the *lgs1* levels in Ma85 (Supplementary Fig. S9A). After treatment with abiotic stress and hormones, the seedlings were allowed to recover for a further 5 d under normal growth conditions. We found that there was a highly significant increase in survival rate in JF178 from cold (4 °C) stress (Fig. 7A, B). We further investigated the time-course of expression patterns of *LGS1* in response to cold treatment, and found that *lgs1* expression was significantly down-regulated (Supplementary Fig. S9B), which was correlated with the up-regulation of *osa-miR396* members except *miR396f*, which was not affected by cold treatment (Supplementary Fig. S9C). After recovery from cold treatment, the expression of *lgs1* and miR396 members returned to normal levels (Supplementary Fig. S9D, E). After cold treatment for 40 min, the expression of *osa-miR396a–osa-miR396e* and *miR396g–osa-miR396i* in Ma85, JF178, and JF178 RNAi plants was enhanced, and the expression of *osa-miR396a–osa-miR396c* in Ma85-expressing *LGS1*[JF178] (MaCP) plants was significantly up-regulated, but *osa-miR396f* was significantly down-regulated (Supplementary Fig. S10A–C). Based on these data, we conclude that the expression of *miR396* members is up-regulated in response to cold stress, which in turn strongly down-regulates *LGS1* transcript levels.

We also treated seedlings of Ma85, JF178, Samba, NIL-*LGS1*[JF178], and SambaRNAi transgenic plants with 4 °C, and then allowed them to grow for a further 5 d under normal growth conditions. We found that the survival rates of the Ma85 seedlings expressing *LGS1*[JF178] (MaCP) after 4 °C treatment for 24, 48, and 72 h were 31.2, 164.1, and 126.2%, respectively, higher than those of Ma85 (Fig. 7C). In contrast, the survival rates of the JF178 seedlings expressing *lgs1*[Ma85] (JFCP) were 36.8, 78.6, and 99.7%, respectively, lower than those of JF178 (Fig. 7C). Furthermore, the survival rates after 4 °C treatment for 24, 48, and 72 h were 15.1, 2.3, and 1.0%, respectively, higher in NIL-*LGS1*[JF178] seedlings, but 70.7, 78.5, and 100% lower in SambaRNAi seedlings, than those in the control Samba (Fig. 7D). Our data also showed that the
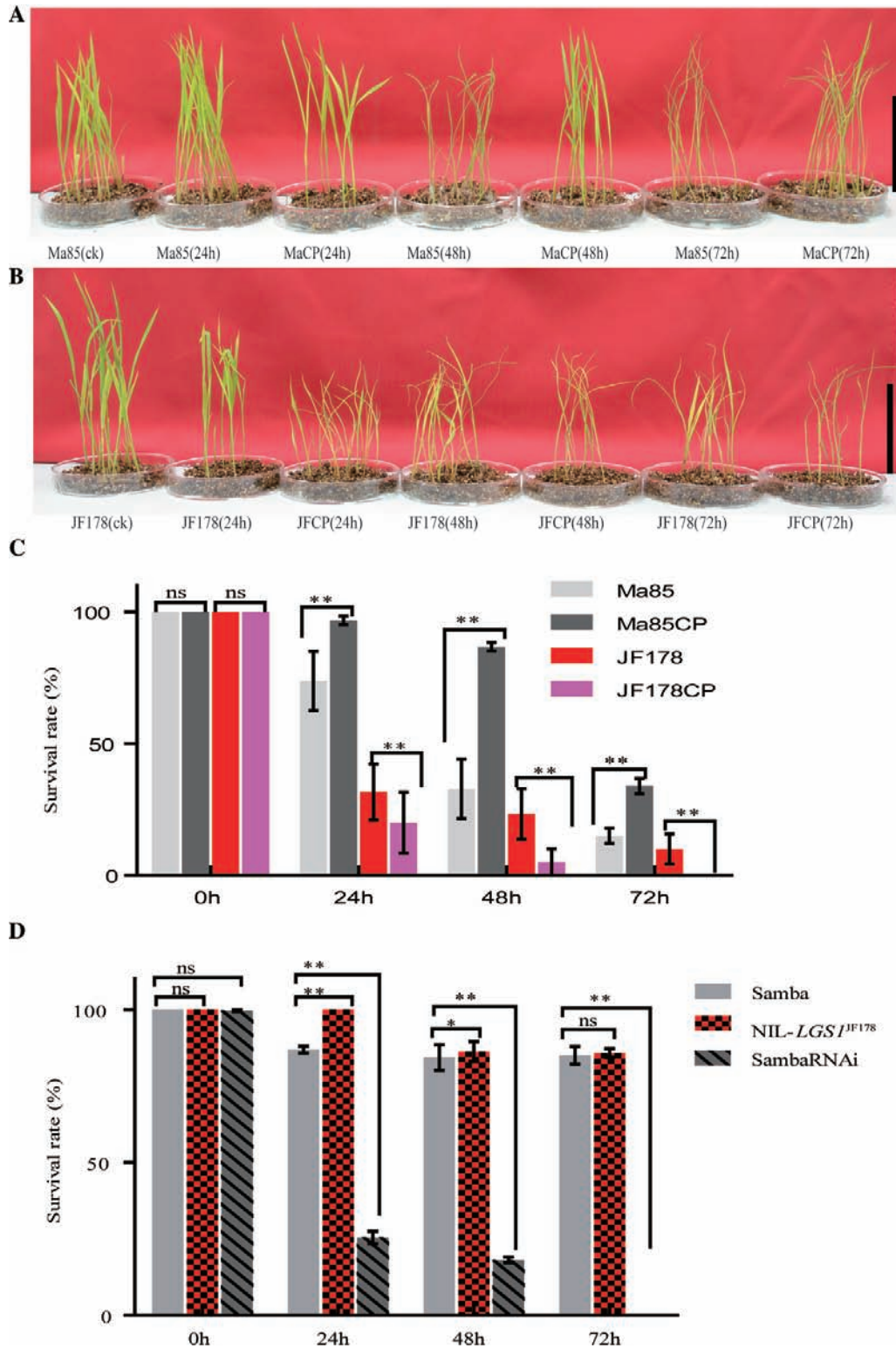
**Fig. 7.** Abiotic stress response of *LGS1*. (A and B) Phenotype of Ma85 and MaCP (A), and JF178 and JFCP (B) after cold (4 °C) treatment (*n*=30). Ma85(ck) and JF178(ck), unstressed controls; MaCP and JFCP, transgenic plants expressing the complementation vector p*LGS1::LGS1* in Ma85 and p*lgs1::lgs1* in JF178, respectively. Plants were treated for 24, 48, and 72 h, respectively. Scale bar=10 cm in (A and B). (C and D) Comparison of survival rates after cold treatment in Ma85, JF178, and transgenic plants expressing the complementation vectors p*LGS1::LGS1* in Ma85 and p*lgs1::lgs1* in JF178, respectively (C), and Samba, NIL-*LGS1*^JF178, and Samba RNAi lines (D). Ma85, JF178, and Samba serve as controls in (C) and (D). Values are given as the mean ±SE. ns *P*>0.05, *\*P*<0.05, **\*\*P*<0.01 were calculated by Student's *t*-test. (This figure is available in colour at *JXB* online.)

expression levels of *lgs1* and miR396 members returned to normal levels (Supplementary Fig. S11A–E) after the removal of cold stress, suggesting that these seedlings had recovered from the cold treatment. Taken together, these data demonstrate that the *LGS1* allele enhances cold tolerance at the seedling stage of rice.

# Discussion

## *A missense mutation in LGS1 results in the development of enlarged grains*

In this study, we cloned and characterized a gain–of–function mutant *LGS1*, and our data demonstrate that a 2 bp substitution (TC to AA) in *LGS1* results in increases in cell length and cell numbers in the longitudinal direction of developing grains and promotes cell expansion in the latitudinal direction. As a result, there is an increase in glume volume and endosperm size in the JF178 mutant that contains the *LGS1* allele. The increase in glume volume was found to be correlated with increases in grain length, grain width, thousand–grain weight, and grain yield in JF178. Analysis of the genetic transformation tests reveals that the elevated *LGS1* mRNA is the cause of the enlarged grains in JF178, indicating that the *LGS1* mRNA level serves as a positive regulator of grain size in rice.

## OsGRF4 *regulates grain formation through interaction with* OsGIF *co-activator*

*LGS1* encodes a plant-specific growth-regulating factor, an allele of *OsGRF4*, also known as *GS2* (Duan *et al.*, 2015; Hu *et al.*, 2015), *GL2* (Che *et al.*, 2015), *PT2* (Sun *et al.*, 2016), and *GLW2* (Li *et al.*, 2016). Similar to *LGS1*, these alleles of *OsGRF4* also positively control grain length, grain width, grain weight, and other traits. The GRF family of transcription factors comprises nine members in *A. thaliana*, and has been shown to regulate leaf cell proliferation and expansion, stress responses, and pistil development (Kim *et al.*, 2003; Rodriguez *et al.*, 2010; Kim *et al.*, 2012; Liang *et al.*, 2014). There are 14 GRF family members in *Zea mays*, some of which have been shown to control the bolting stage and inflorescence stem growth (Zhang *et al.*, 2008). Both the *indica* (Supplementary Fig. S12) and *japonica* subspecies of rice (Choi *et al.*, 2004) have 12 GRF members. Previous observations have shown that GRF family members regulate stem elongation, inflorescence development, and floral organogenesis in plants (Van der Knopp *et al.*, 2000; Choi *et al.*, 2004; Liu *et al.*, 2014; Gao *et al.*, 2015). In general, GRF transcription factor proteins typically contain a QLQ domain and a WRC domain, which are implicated in DNA remodelling and transcription activation. In addition to having these two highly conserved domains, rice LGS1 also includes a transcription activation domain at its C-terminus (Supplementary Fig. S3D–G, I, J). The QLQ domain of GRFs has been shown to bind to the SNH domain of GIFs to form a transcriptional co-activator, which promotes continuous differentiation and generation of new tissues throughout the plant life cycle (Kim and Kende, 2004; Zhang *et al.*, 2008; Liang *et al.*, 2014; Kim and Tsukaya, 2015). Consistent with these reports, our analysis using the yeast system showed that both LGS1 and lgs1 proteins interacted strongly with OsGIF3 (note that OsGIF3 of Supplementary Fig. S12 is designated as OsGIF1 in Duan *et al.*, 2015 and Li *et al.*, 2016). Interestingly, overexpression of *OsGIF1* has previously been found to lead to development of larger and heavier grains than the wild-type variety (Che *et al.*, 2015; Duan *et al.*, 2015; Li *et al.*, 2016). Whether other

*OsGIF* genes also regulate grain size remains to be studied in the future.

## *miR396 members regulate the transcript level of LGS1*

The WRC domain of GRF proteins is highly conserved, and its corresponding mRNA has been believed to be the target of miR396 in plants (Baucher *et al.*, 2013; Kim and Tsukaya, 2015). Most miRNAs exert their functions to down-regulate the expression of target genes, and have been implicated in the regulation of cell differentiation and organogenesis in plants (Liu *et al.*, 2009; Rodriguez *et al.*, 2010; Ercoli *et al.*, 2016; Rodriguez *et al.*, 2016). *miR396b* has been found to mediate *OsGRF6* and regulate rice yield by shaping inflorescence architecture (Gao *et al.*, 2015). *miR396c*, and *g/h/i* may mediate *GS2* (Duan *et al.*, 2015; Hu *et al.*, 2015), *miR396c* mediates *GLW2* (Li *et al.*, 2016), and *miR396d* mediates *GL2* (Che *et al.*, 2015). The role of *miR396* in mediation of GRF transcripts has also been shown by *miR396c* overexpression, which markedly decreases rice grain size and weight (Li *et al.*, 2016). *GRF4^{NGR2}* prevents miR396-mediated cleavage of GRF4 mRNA, thereby increasing GRF4 mRNA and GRF4 abundance, and promoting $NH_4^+$ uptake (Li *et al.*, 2018). Analysis of the *lgs1* (*OsGRF4*) sequence suggested that it could be targeted by all nine miR396 precursors (Supplementary Table S7; Supplementary Fig. S8A). The expression levels of *OsmiR396* were also found to correlate with a regulatory network of *OsGRF4*. Thus, the expression of *OsmiR396* members could significantly attenuate the transcript level of *lgs1* (Supplementary Fig. S8B). The mutation in *LGS1* appeared to prevent cleavage by miR396, which led to an elevated transcript level of *LGS1*, resulting in the formation of enlarged grains in the mutant line JF178. Taken together, these findings indicate that *miR396* regulates the transcript level of *OsGRF4* (*lgs1*) in an antagonistic manner and the 2 bp mutation of *LGS1* impedes the down-regulation of *LGS1* transcripts by *miR396*.

## *LGS1 improves cold tolerance of rice seedlings*

Transcription factors have been implicated widely in the regulation of signaling and metabolic pathways in response to adversity stress, including biotic stress (bacterial pathogens, fungi, and insects) and abiotic stress (heavy metals, high temperatures, low temperatures, drought, waterlogging, high salinity, and high alkalinity). The pathways of stress responses overlap extensively in plants (Singh *et al.*, 2002; Nakashima *et al.*, 2009; Brotman *et al.*, 2012; Ambavaram *et al.*, 2014). The regulation of gene expression via miRNAs is one of the mechanisms involved in the different stress responses. Plants produce crosstalk signal responses that regulate cellular physiology and metabolism, and ultimately yield formation in crops (Jones-Rhoades and Bartel, 2004; Ding *et al.*, 2011; Ambavaram *et al.*, 2014). Previous studies on the *OsGRF* gene–*miR396* stress networks in rice have shown that *OsGRF4* is down-regulated by drought, overexpression of *miR396c* leads to a decrease in salt and alkali stress tolerance, and the expression of *miR396d* is down-regulated by cadmium stress (Gao *et al.*, 2010; Ding *et al.*,
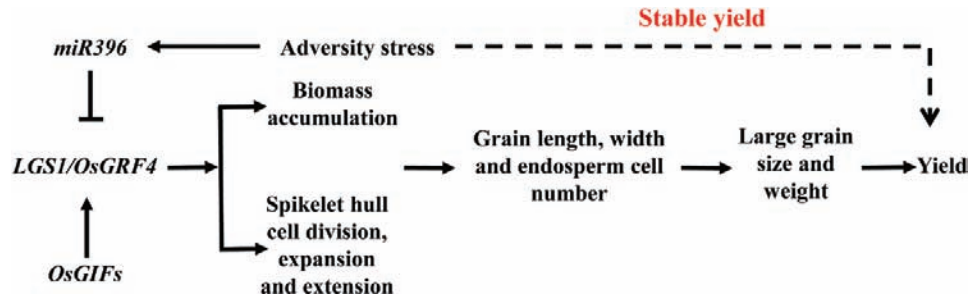
**Fig. 8.** Schematic model for the role of *LGS1* in the regulation of grain length, grain width, and grain weight. LGS1 forms a protein complex with OsGIF to regulate gene expression. The transcript level of *LGS1* is regulated by *miR396*. *LGS1* promotes cell division, cell extension, and cell expansion, resulting in increases in vegetative biomass and spikelet glume volume. During grain development, *LGS1* enhances the grain filling rate and increases grain length and endosperm cell numbers, leading to the production of enlarged grains and higher yield in rice. Furthermore, the expression of *miR396* is up-regulated by stress, which in turn reduces the transcript level of *lgs1*. The nucleotide substitution in *LGS1* prevents regulation of *LGS1* by *miR396* and allows the *LGS1* transcript to accumulate during adversity stress, which improves stress tolerance in rice seedlings.

2011; Tang and Chu, 2017). OsGRF4 and GL2 transcription activation activity is known to be down-regulated by GSK2 to a large extent and functions in the brassinosteroid signaling pathway (Che *et al.*, 2015), which has been shown to be cold stress responsive in Arabidopsis (Li *et al.*, 2017). In this study, we observed that *OsGRF4* may be involved in the signaling pathways of hormone and stress responses (Supplementary Fig. S9A). Although the stress response patterns were highly complex, the mutation in *LGS1* significantly enhanced tolerance to low temperatures and increased the survival rates of seedlings after recovery (Fig. 7). This conclusion is consistent with the observation that the transcript levels of *lgs1* were down-regulated by cold treatment, whereas *OsmiR396* expression was up-regulated by low temperatures (Supplementary Figs S9B, C, S10). Taken together, these results indicate that *miR396* acts as a negative regulator to target *OsGRF4* for cleavage and mediate plant stress responses. This study identified the missense mutation of *LGS1* as the interfering site that breaks the antagonistic regulation pattern of *OsGRF4–miR396* stress response networks, resulting in the development of large grains and the enhancement of cold tolerance in rice.

In summary, this work has identified an important gene that regulates grain development and stress tolerance in rice. We propose a model to elucidate the possible mechanism of *LGS1* in the regulation of rice growth and development, including grain and yield formation and adaptability to stress environments (Fig. 8). The results presented in this report provide new insight into a new genetic regulation mechanism of the *OsGRF4–OsGIF–OsmiR396* stress response network. This model contributes to the understanding of the complex regulatory mechanisms underlying seed development and yield formation in rice and other crops, and could be useful for applications in molecular breeding and molecular marker–assisted selection breeding in rice.

## Supplementary data

Fig. S1. Construction of the near-isogenic line NIL-*LGS1*.
Fig. S2. Panicle phenotype analysis of *LGS1*.
Fig. S3. *LGS1* expression vector constructs, subcellular localization, and interaction partner.
Fig. S4. Grain shape traits of transgenic plants.

Fig. S5. Glume cell number, endosperm size, and grain filling dynamics of NILs.
Fig. S6. Biomass accumulation of NILs.
Fig. S7. Response of NILs to plant hormone treatments.
Fig. S8. Targeting of the *LGS1* and *lgs1* mRNAs by miR396.
Fig. S9. Expression levels of *LGS1* and miR396 in response to low temperature stress.
Fig. S10. Expression levels of *miR396* members in Ma85, JF178, Samba, and transgenic lines in response to cold treatment.
Fig. S11. Expression levels of *LGS1* and miR396 in rice seedlings after recovery from cold treatment.
Fig. S12. Phylogenetic tree of the GRF family members in rice.
Table S1. Sequences of primers for vector construction and PCR analysis.
Table S2. Polymorphisms of the *LGS1* coding sequence in different accessions.
Table S3. Polymorphisms of the *LGS1* non-coding sequence in different accessions.
Table S4. Young panicle differentiation stage of rice.
Table S5. RNA-seq analysis of cell cycle genes in NILs.
Table S6. RNA-seq analysis of unknown cell cycle, expansin, and extensin genes in NILs.
Table S7. Alignment sites of the miR396 target in *OsGRF4*.

## Acknowledgements

## References

**Abe A, Kosugi S, Yoshida K, *et al.*** 2012. Genome sequencing reveals agronomically important loci in rice using MutMap. Nature Biotechnology **30**, 174–178.

**Ambavaram MM, Basu S, Krishnan A, Ramegowda V, Batlang U, Rahman L, Baisakh N, Pereira A.** 2014. Coordinated regulation of

photosynthesis in rice increases yield and tolerance to environmental stress. Nature Communications **5**, 5302.

**Baucher M, Moussawi J, Vandeputte OM, Monteyne D, Mol A, Pérez-Morga D, El Jaziri M.** 2013. A role for the miR396/GRF network in specification of organ type during flower development, as supported by ectopic expression of *Populus trichocarpa* miR396c in transgenic tobacco. Plant Biology **15**, 892–898.

**Brotman Y, Lisec J, Méret M, Chet I, Willmitzer L, Viterbo A.** 2012. Transcript and metabolite analysis of the *Trichoderma*-induced systemic resistance response to *Pseudomonas syringae* in *Arabidopsis thaliana*. Microbiology **158**, 139–146.

**Che R, Tong H, Shi B, et al.** 2015. Control of grain size and rice yield by GL2-mediated brassinosteroid responses. Nature Plants **2**, 15195.

**Choi D, Kim JH, Kende H.** 2004. Whole genome analysis of the OsGRF gene family encoding plant-specific putative transcription activators in rice (*Oryza sativa* L.). Plant & Cell Physiology **45**, 897–904.

**Cui Y, Rao S, Chang B, et al.** 2015. AtLa1 protein initiates IRES-dependent translation of WUSCHEL mRNA and regulates the stem cell homeostasis of Arabidopsis in response to environmental hazards. Plant, Cell & Environment **38**, 2098–2114.

**Ding Y, Chen Z, Zhu C.** 2011. Microarray-based analysis of cadmium-responsive microRNAs in rice (*Oryza sativa*). Journal of Experimental Botany **62**, 3563–3573.

**Duan P, Ni S, Wang J, Zhang B, Xu R, Wang Y, Chen H, Zhu X, Li Y.** 2015. Regulation of OsGRF4 by OsmiR396 controls grain size and yield in rice. Nature Plants **2**, 15203.

**Ercoli MF, Rojas AM, Debernardi JM, Palatnik JF, Rodriguez RE.** 2016. Control of cell proliferation and elongation by miR396. Plant Signaling & Behavior **11**, e1184809.

**Gao F, Wang K, Liu Y, et al.** 2015. Blocking miR396 increases rice yield by shaping inflorescence architecture. Nature Plants **2**, 15196.

**Gao P, Bai X, Yang L, Lv D, Li Y, Cai H, Ji W, Guo D, Zhu Y.** 2010. Over-expression of osa-MIR396c decreases salt and alkali stress tolerance. Planta **231**, 991–1001.

**Godfray HC, Beddington JR, Crute IR, Haddad L, Lawrence D, Muir JF, Pretty J, Robinson S, Thomas SM, Toulmin C.** 2010. Food security: the challenge of feeding 9 billion people. Science **327**, 812–818.

**Hiei Y, Ohta S, Komari T, Kumashiro T.** 1994. Efficient transformation of rice (*Oryza sativa* L.) mediated by *Agrobacterium* and sequence analysis of the boundaries of the T-DNA. The Plant Journal **6**, 271–282.

**Hu J, Wang Y, Fang Y, et al.** 2015. A rare allele of GS2 enhances grain size and grain yield in rice. Molecular Plant **8**, 1455–1465.

**Huang R, Jiang L, Zheng J, Wang T, Wang H, Huang Y, Hong Z.** 2013. Genetic bases of rice grain shape: so many genes, so little known. Trends in Plant Science **18**, 218–226.

**Huang X, Zhao Y, Wei X, et al.** 2011. Genome-wide association study of flowering time and grain yield traits in a worldwide collection of rice germplasm. Nature Genetics **44**, 32–39.

**Jefferson RA, Kavanagh TA, Bevan MW.** 1987. GUS fusions: β-glucuronidase as a sensitive and versatile gene fusion marker in higher plants. The EMBO Journal **6**, 3901–3907.

**Jones-Rhoades MW, Bartel DP.** 2004. Computational identification of plant microRNAs and their targets, including a stress-induced miRNA. Molecular Cell **14**, 787–799.

**Jones-Rhoades MW, Bartel DP, Bartel B.** 2006. MicroRNAs and their regulatory roles in plants. Annual Review of Plant Biology **57**, 19–53.

**Kim D, Pertea G, Trapnell C, Pimentel H, Kelley R, Salzberg SL.** 2013. TopHat2: accurate alignment of transcriptomes in the presence of insertions, deletions and gene fusions. Genome Biology **14**, R36.

**Kim JH, Choi D, Kende H.** 2003. The AtGRF family of putative transcription factors is involved in leaf and cotyledon growth in Arabidopsis. The Plant Journal **36**, 94–104.

**Kim JH, Kende H.** 2004. A transcriptional coactivator, AtGIF1, is involved in regulating leaf growth and morphology in Arabidopsis. Proceedings of the National Academy of Sciences, USA **101**, 13374–13379.

**Kim JH, Tsukaya H.** 2015. Regulation of plant growth and development by the GROWTH-REGULATING FACTOR and GRF-INTERACTING FACTOR duo. Journal of Experimental Botany **66**, 6093–6107.

**Kim JS, Mizoi J, Kidokoro S, et al.** 2012. Arabidopsis growth-regulating factor7 functions as a transcriptional repressor of abscisic acid- and osmotic stress-responsive genes, including DREB2A. The Plant Cell **24**, 3393–3405.

**Lan Y, Su N, Shen Y, et al.** 2012. Identification of novel miRNAs and miRNA expression profiling during grain development in indica rice. BMC Genomics **13**, 264.

**Li H, Ye K, Shi Y, Cheng J, Zhang X, Yang S.** 2017. BZR1 positively regulates freezing tolerance via CBF-dependent and CBF-independent pathways in Arabidopsis. Molecular Plant **10**, 545–559.

**Li S, Gao F, Xie K, et al.** 2016. The OsmiR396c–OsGRF4–OsGIF1 regulatory module determines grain size and yield in rice. Plant Biotechnology Journal **14**, 2134–2146.

**Li S, Tian Y, Wu K, et al.** 2018. Modulating plant growth–metabolism coordination for sustainable agriculture. Nature **560**, 595–600.

**Liang G, He H, Li Y, Wang F, Yu D.** 2014. Molecular mechanism of microRNA396 mediating pistil development in Arabidopsis. Plant Physiology **164**, 249–258.

**Liu D, Song Y, Chen Z, Yu D.** 2009. Ectopic expression of miR396 suppresses GRF target gene expression and alters leaf growth in Arabidopsis. Physiologia Plantarum **136**, 223–236.

**Liu H, Guo S, Xu Y, Li C, Zhang Z, Zhang D, Xu S, Zhang C, Chong K.** 2014. OsmiR396d-regulated OsGRFs function in floral organogenesis in rice through binding to their targets OsJMJ706 and OsCR4. Plant Physiology **165**, 160–174.

**Liu S, Hua L, Dong S, Chen H, Zhu X, Jiang J, Zhang F, Li Y, Fang X, Chen F.** 2015. OsMAPK6, a mitogen-activated protein kinase, influences rice grain size and biomass production. The Plant Journal **84**, 672–681.

**Nakashima K, Ito Y, Yamaguchi-Shinozaki K.** 2009. Transcriptional regulatory networks in response to abiotic stresses in Arabidopsis and grasses. Plant Physiology **149**, 88–95.

**Okuley J, Lightner J, Feldmann K, Yadav N, Lark E, Browse J.** 1994. Arabidopsis FAD2 gene encodes the enzyme that is essential for polyunsaturated lipid synthesis. The Plant Cell **6**, 147–158.

**Rodriguez RE, Ercoli MF, Debernardi JM, Breakfield NW, Mecchia MA, Sabatini M, Cools T, De Veylder L, Benfey PN, Palatnik JF.** 2015. MicroRNA miR396 regulates the switch between stem cells and transit-amplifying cells in Arabidopsis roots. The Plant Cell **27**, 3354–3366.

**Rodriguez RE, Mecchia MA, Debernardi JM, Schommer C, Weigel D, Palatnik JF.** 2010. Control of cell proliferation in *Arabidopsis thaliana* by microRNA miR396. Development **137**, 103–112.

**Rodriguez RE, Schommer C, Palatnik JF.** 2016. Control of cell proliferation by microRNAs in plants. Current Opinion in Plant Biology **34**, 68–76.

**Singh K, Foley RC, Oñate-Sánchez L.** 2002. Transcription factors in plant defense and stress responses. Current Opinion in Plant Biology **5**, 430–436.

**Smith NA, Singh SP, Wang MB, Stoutjesdijk PA, Green AG, Waterhouse PM.** 2000. Total silencing by intron-spliced hairpin RNAs. Nature **407**, 319–320.

**Stoutjesdijk PA, Singh SP, Liu Q, Hurlstone CJ, Waterhouse PA, Green AG.** 2002. hpRNA-mediated targeting of the Arabidopsis FAD2 gene gives highly efficient and stable silencing. Plant Physiology **129**, 1723–1731.

**Sun P, Zhang W, Wang Y, He Q, Shu F, Liu H, Wang J, Wang J, Yuan L, Deng H.** 2016. OsGRF4 controls grain shape, panicle length and seed shattering in rice. Journal of Integrative Plant Biology **58**, 836–847.

**Tang J, Chu C.** 2017. MicroRNAs in crop improvement: fine-tuners for complex traits. Nature Plants **3**, 17077.

**Trapnell C, Williams BA, Pertea G, Mortazavi A, Kwan G, van Baren MJ, Salzberg SL, Wold BJ, Pachter L.** 2010. Transcript assembly and quantification by RNA-Seq reveals unannotated transcripts and isoform switching during cell differentiation. Nature Biotechnology **28**, 511–515.

**Van der Knapp E, Kim JH, Kende H.** 2000. A novel gibberellin-induced gene from rice and its potential regulatory role in stem growth. Plant Physiology **122**, 695–704.

**Wang S, Li S, Liu Q, et al.** 2015. The OsSPL16–GW7 regulatory module determines grain shape and simultaneously improves rice yield and grain quality. Nature Genetics **47**, 949–954.

**Wang Y, Xiong G, Hu J, et al.** 2015. Copy number variation at the GL7 locus contributes to grain size diversity in rice. Nature Genetics **47**, 944–948.

**Wesley SV, Helliwell CA, Smith NA, et al.** 2001. Construct design for efficient, effective and high-throughput gene silencing in plants. The Plant Journal **27**, 581–590.

**Wu W, Liu X, Wang M, *et al.*** 2017. A single-nucleotide polymorphism causes smaller grain size and loss of seed shattering during African rice domestication. Nature Plants **3**, 17064.

**Zhang D, Li B, Jia G, Zhang T, Dai J, Li J, Wang S.** 2008. Isolation and characterization of genes encoding GRF transcription factors and GIF transcriptional coactivators in maize (*Zea mays* L.). Plant Science **175**, 809–817.

**Zhao K, Tung CW, Eizenga GC, *et al.*** 2011. Genome-wide association mapping reveals a rich genetic architecture of complex traits in *Oryza sativa*. Nature Communications **2**, 467.